Electronic Supporting Information

A Multi-Functional Two-Dimensional Zn(II)-Organic Framework for Selective Carbon Dioxide Adsorption, Sensing of Nitrobenzene and $Cr_2O_7^{2-}$

Qi Wu, Xiao-Li Yang, Ze-Yu Ding, Xiao-Yun Meng, Wen-Yan Zhang,* Yang-Tian Yan,* Guo-Ping Yang, and Yao-Yu Wang

[a] Key Laboratory of Synthetic and Natural Functional Molecule of Ministry of Education, Shaanxi Key Laboratory of Physico-Inorganic Chemistry, College of Chemistry & Materials Science, and, School of Chemical Engineering, Northwest University, Xi'an 710127, P. R. China.

[b] School of Materials Science & Engineering, Xi'an Polytechnic University, Xi'an 710048, P. R. China.

Table S1. Bond lengths [Å] and angles [°]

1	
Zn(1)-O(1)	1.948(4)
Zn(1)-O(3)#1	1.959(4)
Zn(1)-O(5)#2	1.955(4)
Zn(1)-N(1)#3	2.037(5)
O(1)-Zn(1)-O(3)#1	117.41(18)
O(1)-Zn(1)-O(5)#2	116.12(17)
116.12(17)	107.11(18)
O(3)#1-Zn(1)-N(1)#3	99.75(19)
O(5)#2-Zn(1)-O(3)#1	104.89(18)
O(5)#2-Zn(1)-N(1)#3	110.30(18)

Symmetry transformations used to generate equivalent atoms: #1: x+1/2, -y+3/2, z+1/2; #2: x, y+1, z; #3: -x+3/2, y+1/2, -z+3/2; #4: x-1/2, -y+3/2, z-1/2; #5: x,y-1,z; #6: -x+3/2, y-1/2, -z+3/2.

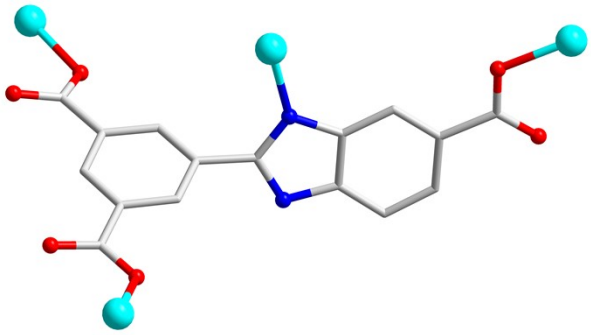

Fig. S1. The coordination modes of L^{3-} ligands in **1**.

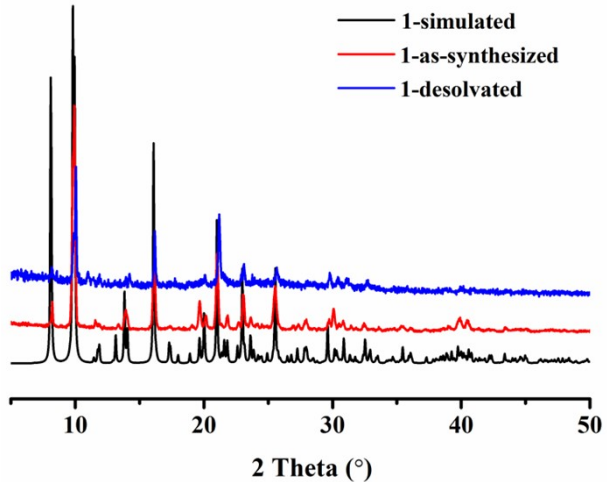

Fig. S2. PXRD patterns of **1**

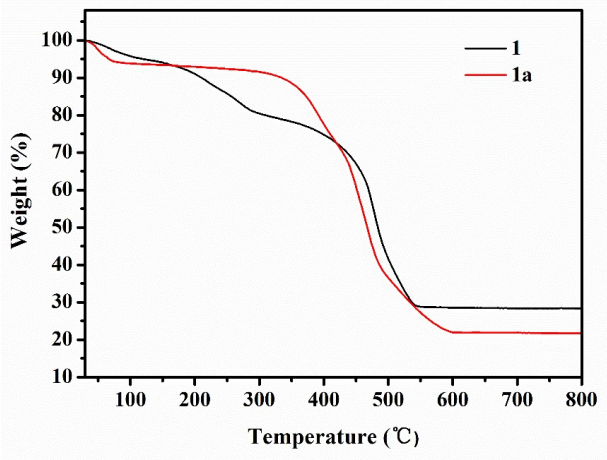

Fig. S3. TGA curves of the as-synthesized **1** and desolvated sample **1a**.

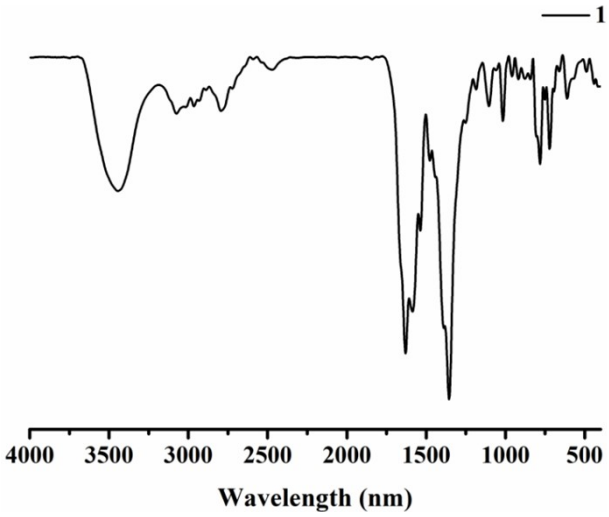

Fig. S4. The FT-IR spectra of the as synthesized **1**.

IAST adsorption selectivity calculation

The experimental isotherm data for pure CO_2 and CH_4 (measured at 273 and 298 K) were fitted using a Langmuir-Freundlich (L-F) model

$$q = \frac{a * b * p^c}{1 + b * p^c}$$

Where q and p are adsorbed amounts and pressures of component i, respectively. The adsorption selectivities for binary mixtures of CO_2/CH_4 at 273 and 298 K, defined by

$$S_{ads} = (q_1/q_2)/(p_1/p_2)$$

Where q_i is the amount of i adsorbed and p_i is the partial pressure of i in the mixture.

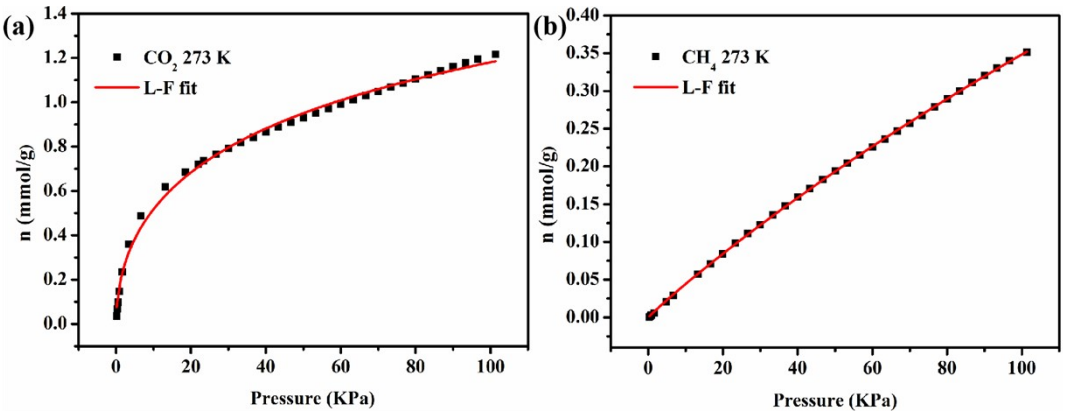

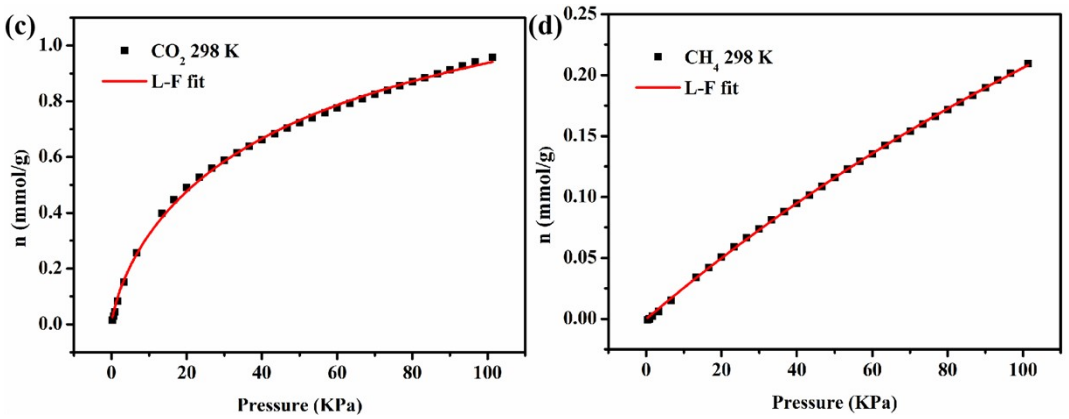

Fig. S5. (a) CO_2 adsorption isotherms of **1a** at 273K with fitting by L-F model: a = 2.68891, b = 0.07262, c = 0.51606, Chi^2 = 5.51534E-4, R^2 = 0.99552; (b) CH_4 adsorption isotherms of **1a** at 273 K with fitting by L-F model: a = 2.29251, b = 0.00215, c = 0.96041, Chi^2 = 1.29167E-6, R^2 = 0.99990; (c) CO_2 adsorption isotherms of **1a** at 298K with fitting by L-F model: a = 1.58553, b = 0.04502, c = 0.75334, Chi^2 =1.04563E- , R^2 = 0.99876; (d) CH_4 adsorption isotherms of **1a** at 298K with fitting by L-F model: a = 0.8808, b = 0.0029, c = 1.01126, Chi^2 = 1.36911E-6, R^2 = 0.9997.

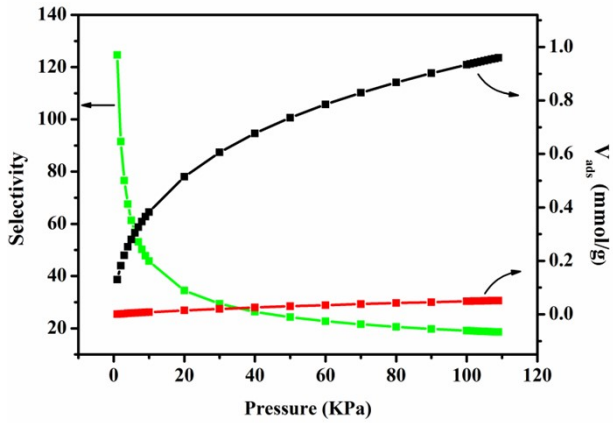

Fig. S6. IAST adsorption selectivities of **1a** for the equimolar mixture of CO_2 and CH_4 (50:50) at 273 K.

Calculation of sorption heat for CO_2 uptake using Virial-II mode

$$\ln P = \ln N + 1/T\sum_{i=0}^{m} a_i N^i + \sum_{i=0}^{n} b_i N^i \qquad Q_{st} = -R\sum_{i=0}^{m} a_i N^i$$

The above equation was applied to fit the combined CO_2 isotherm data for desolvated **1a** at 273 and 298 K, where P is the pressure, N is the adsorbed amount, T is the temperature, a_i and b_i are virial coefficients, and m and n are the number of coefficients

used to describe the isotherms. Q_{st} is the coverage-dependent enthalpy of adsorption and R is the universal gas constant.

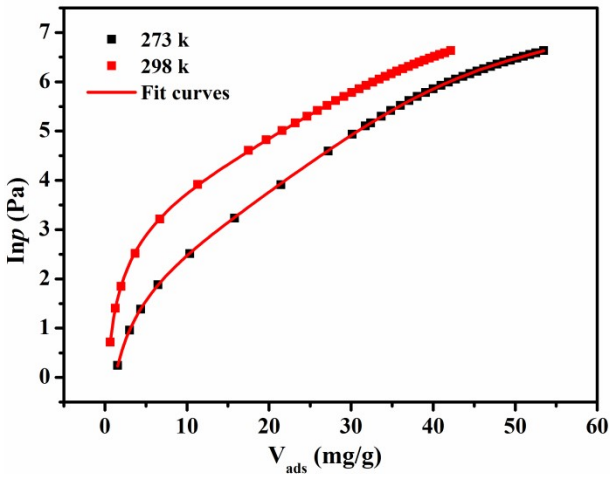

Fig. S7. Virial analysis of the CO_2 adsorption data at 273 and 298 K for **1a**.
Fitting results: a_0= -4527.98711, a_1 = 41.0419, a_2 = 0.01962, a_3 = 0.03776, a_4 = -9.12027E-4, a_5 = 6.56488E-6; b_0 = 16.3151, b_1 = -0.10336, b_2 = -0.00145; Chi^2 = 9.82062E-5, R^2 = 0.99996.

Table S2. Comparison of K_{sv} values and/or detecting limits between **1** and the selected MOFs for nitrobenzene.

Entry	MOFs	K_{sv}/M^{-1}	Detecting limits/M	Media	Ref
1	$[Zn(HNTB)(phen)]_n$	60.75	7.53×10^{-4}	DMF	1
2	$[Tb(L_1)(H_2O)_2]\cdot$guest	589.6		N-hexane	2
3	$[Tb(L_2)(H_2O)_2]\cdot$guest	445.5			
4	$[Zn_3(TTPA)_2(DHTP)_3]\cdot2DMF$	1.86×10^2		Ethanol	3
5	$\{[Tb_2(L)_3(H_2O)4]\cdot10H_2O\}_n$	1.8×10^3		DMF	4
6	**1**	1.88×10^3	6.38×10^{-4}	DMF	This work
7	$[Zn(H_2L^{2-})(H_2O)]n$	3.26×10^3		DMF	5
8	$[Zn(tba)_2]\cdot$DMA	8.58×10^3	8.33×10^{-5}	DMF	6
9	$[Eu_2(MPDA)_3(H_2O)_2]\cdot2H_2O$	1.033×10^4	5.69×10^{-6}	Ethanol	7
10	$\{[Tb(DMTDC)_{1.5}(H_2O)_2]\bullet DEF\}_n$	1.69×10^4		DMF	8
11	$[Pb_2(2\text{-}NCP)_2(L_1)]_n$	1.62×10^7	4.0×10^{-10}	H_2O	9

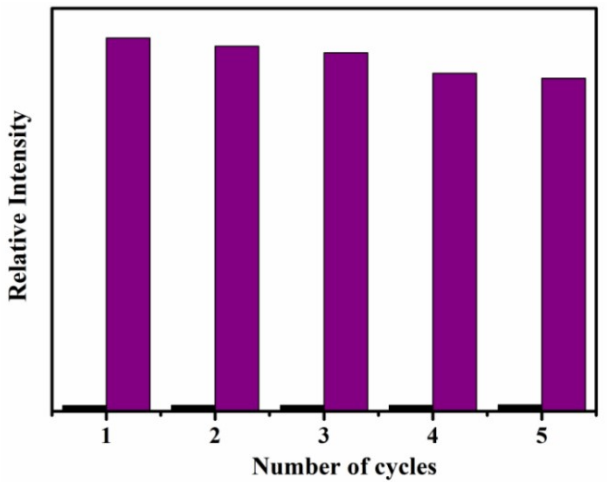

Fig. S8. Recoverable fluorescence intensity of **1** in recyclable experiments for nitrobenzene.

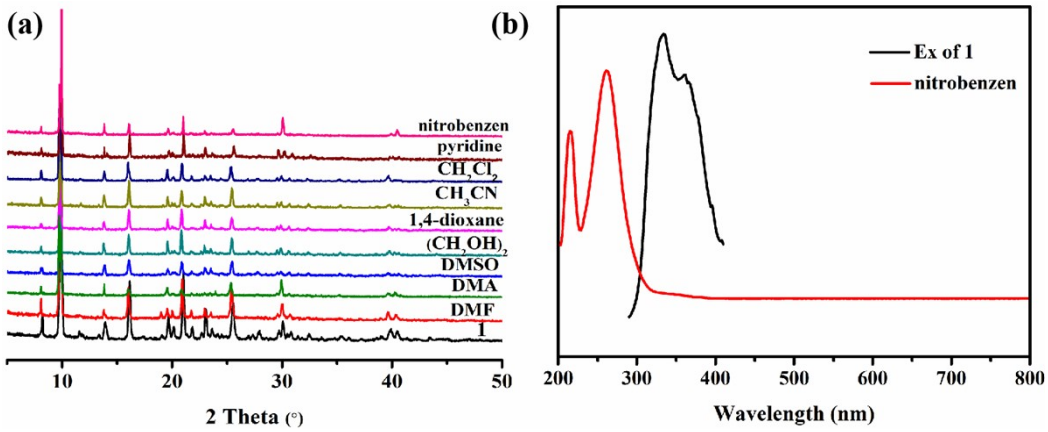

Fig. S9 (a) PXRD patterns of **1** treated by different small organic solvents. (b) UV-vis absorption spectra of nitrobenzene, and the excitation spectrum of **1.**

Table S3. Comparison of K_{sv} values and/or detecting limits between **1** and the selected MOFs for $Cr_2O_7^{2-}$ ion.

Entry	MOFs	K_{sv}/M^{-1}	Detecting limits/M	Media	Ref.
1	$[Zn(OBA)_2(L_1)\cdot 2DMA]_n$	1.89×10^3	2.37×10^{-9}	H_2O	10
2	$\{[Eu(dpc)(2H_2O)]\cdot(Hbibp)_{0.5}\}_n$(VI)	3.97×10^3	1.01×10^{-5}	DMF	11
3	**1**	4.09×10^3	3.6×10^{-4}	DMF	This work
4	$\{[Zn_2(Hbtc)_2(BTD\text{-}bpy)(MeOH)_2]\cdot MeOH\}_n$	6.12×10^3	2.38×10^{-3}	H_2O	12
5	$\{[Cd_3(HL)_2(H_2O)_3]\cdot 3H_2O\cdot 2CH_3CN\}_n$	6.99×10^3	1.17×10^{-4}	H_2O	13
6	$[Zn(pdca)(bbibp)_{0.5}]_n$	8.05×10^3	3.7×10^{-6}	H_2O	14

7	{[Zn_2(1,4-ndc)$_2$(BTD-bpy)]·0.5MeOH·H_2O}$_n$	8.94×10^3	0.75×10^{-3}	H_2O	12
8	[Zn_2(tpeb)(bpdc)$_2$]	1.12×10^4	1.04×10^{-3}	H_2O	15
9	[Zn(L)$_2$]·2DMF	1.25×10^4	1.45×10^{-3}	H_2O	16
10	[Cd(bipy)][HL]$_n$	2.70×10^5		H_2O	17
11	Cu(II)-tpt-on-Cu(I)-tpt membran	2.22×10^5		H_2O	18

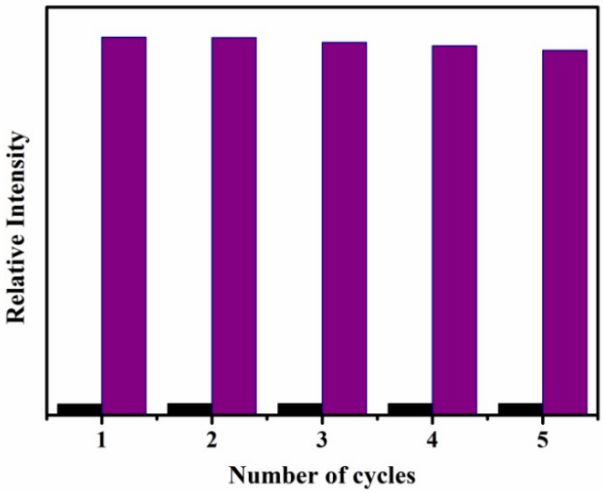

Fig. S10. Recoverable fluorescence intensity of **1** in recyclable experiments for $Cr_2O_7^{2-}$ ion.

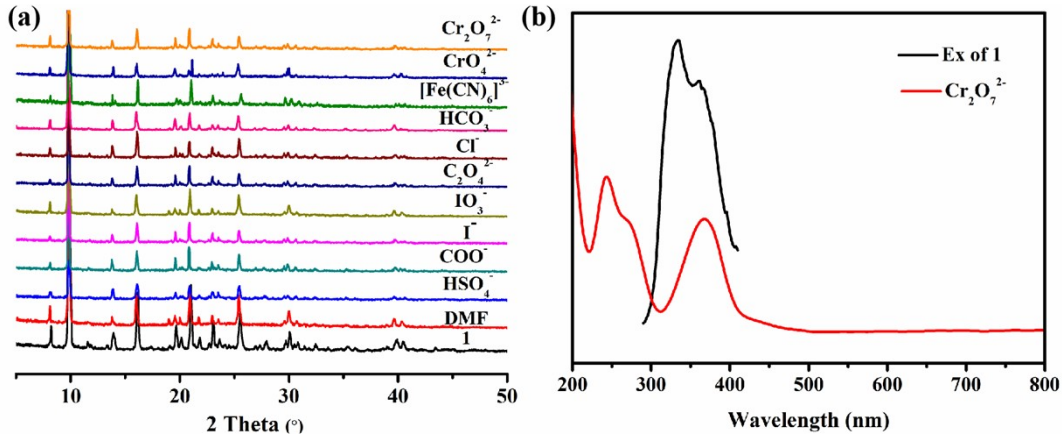

Fig. S11 (a) PXRD patterns of **1** treated by different various anions. (b) UV-vis absorption spectra of $Cr_2O_7^{2-}$ ion, and the excitation spectrum of **1**

References

1. H. Y. Yang, D. Y. Qi, Z. Z. Chen, M. Y. Cao, Y. J. Deng, Z. X. Liu, C. Y. Shao and L. R. Yang, *J. Solid State Chem.*, 2021, **296**, 121970.

2. H. J. Wang, F. J. Cheng, C. C. Zou, Q. Q. Li, Y. Y. Hua, J. G. Duan and W. Q. Jin, *CrystEngComm.*, 2016, **18**, 5639-5646.

3. C. M. Ngue, M. K. Leung and K. L. Lu, *Inorg. Chem.*, 2020, **59**, 2997-3003.

4. Z. Sun, P. Hu, Y. Ma and L. Li, *Dyes. Pigment.*, 2017, **143**, 10-17.

5. Q. Zhao and C. D. Si, *Cryst. Res. Technol.*, 2019, **54**, 1800155.

6. X. D. Fang, J. Yao, R. Fan, X. F. Bai, Y. E. Liu, C. F. Hou, Q. Q. Xu, A. X. Zhu and B. Huang, *J. Solid State Chem.*, 2021, **294**, 121854.

7. S. L. Sun, X. Y. Sun, Q. Sun, E. Q. Gao, J. L. Zhang and W. J. Li, *J. Solid State Chem.*, 2020, **292**, 121701.

8. A. Li, L. Li, Z. Lin, L. Song, Z. H. Wang, Q. Chen, T. Yang, X. H. Zhou, H. P. Xiao and X. J. Yin, *New J. Chem.*, 2015, **39**, 2289-2295.

9. Y. Qiao, J. Guo, D. Li, H. Li, X. Xue, W. Jiang, G. Che and W. Guan, *J. Solid State Chem.*, 2020, **290**, 121610.

10. B. Qin, X. Y. Zhang, J. J. Qiu, G. Gahungu, H. Y. Yuan and J. P. Zhang, *Inorg. Chem.*, 2021, **60**, 1716-1725.

11. Y. Du, H. Yang, R. Liu, C. Shao and L. Yang, *Dalton Trans.*, 2020, **49**, 13003-13016.

12. Q. J. Jiang, J. Y. Lin, Z. J. Hu, V. K. S. Hsiao, M. Y. Chung and J. Y. Wu, *Cryst. Growth Des.*, 2021, **21**, 2056-2067.

13. W. Q. Tong, W. N. Liu, J. G. Cheng, P. F. Zhang, G. P. Li, L. Hou and Y. Y. Wang, *Dalton Trans.*, 2018, **47**, 9466-9473.

14. D. M. Zhang, C. G. Xu, Y. Z. Liu, C. B. Fan, B. Zhu and Y. H. Fan, *J. Solid State Chem.*, 2020, **290**, 121549.

15. B. B. Rath and J. J. Vittal, *Inorg. Chem.*, 2020, **59**, 8818-8826.

16. B. Li, Q. Q. Yan and G. P. Yong, *J. Mater. Chem. C*, 2020, **8**, 11786-11795.

17. W. Q. Kan and S. Z. Wen, *Dyes. Pigment.*, 2017, **139**, 372-380.

18. K. Zhu, R. Fan, J. Wu, B. Wang, H. Lu, X. Zheng, T. Sun, S. Gai, X. Zhou and Y. Yang, *ACS Appl. Mater. Inter.*, 2020, **12**, 58239-58251.